Research Article

Molecular Imaging, Pharmacokinetics, and Dosimetry of ^{111}In-AMBA in Human Prostate Tumor-Bearing Mice

Chung-Li Ho,[1] I-Hsiang Liu,[1] Yu-Hsien Wu,[1] Liang-Cheng Chen,[1] Chun-Lin Chen,[1] Wan-Chi Lee,[1] Cheng-Hui Chuang,[1] Te-Wei Lee,[1] Wuu-Jyh Lin,[1, 2] Lie-Hang Shen,[1] and Chih-Hsien Chang[1, 2]

[1] *Isotope Application Division, Institute of Nuclear Energy Research, Taoyuan 32546, Taiwan*
[2] *Department of Biomedical Imaging and Radiological Sciences, National Yang-Ming University, Taipei 11221, Taiwan*

Correspondence should be addressed to Chih-Hsien Chang, chchang@iner.gov.tw

Molecular imaging with promise of personalized medicine can provide patient-specific information noninvasively, thus enabling treatment to be tailored to the specific biological attributes of both the disease and the patient. This study was to investigate the characterization of DO3A-CH$_2$CO-G-4-aminobenzoyl-Q-W-A-V-G-H-L-M-NH$_2$ (AMBA) *in vitro*, MicroSPECT/CT imaging, and biological activities of ^{111}In-AMBA in PC-3 prostate tumor-bearing SCID mice. The uptake of ^{111}In-AMBA reached highest with $3.87 \pm 0.65\%$ ID/g at 8 h. MicroSPECT/CT imaging studies suggested that the uptake of ^{111}In-AMBA was clearly visualized between 8 and 48 h postinjection. The distribution half-life ($t_{1/2\alpha}$) and the elimination half-life ($t_{1/2\beta}$) of ^{111}In-AMBA in mice were 1.53 h and 30.7 h, respectively. The C_{max} and AUC of ^{111}In-AMBA were 7.57% ID/g and 66.39 h*% ID/g, respectively. The effective dose appeared to be 0.11 mSv/MBq^{-1}. We demonstrated a good uptake of ^{111}In-AMBA in the GRPR-overexpressed PC-3 tumor-bearing SCID mice. ^{111}In-AMBA is a safe, potential molecular image-guided diagnostic agent for human GRPR-positive tumors, ranging from simple and straightforward biodistribution studies to improve the efficacy of combined modality anticancer therapy.

1. Introduction

Prostate cancer is estimated to rank first in number of cancer cases and second in number of deaths due to cancer among men in the Western world [1]. Gastrin-releasing peptides (GRPs), including Bombesin-like peptides (BLPs), are involved in the regulation of a large number of biological processes in the gut and central nervous system (CNS) [2]. They mediate their action on cells by binding to members of a superfamily of G protein-coupled receptors [3]. There are four known subtypes of BN-related peptide receptors, namely, gastrin-releasing peptide receptor (GRPR, BB2, BRS-2), neuromedin B receptor (NMBR, BB1, BRS-1), orphan receptor (BRS-3), and amphibian receptor (BB4-R) [4]. Except the BB4-R, all the receptors were widely distributed, especially in the gastrointestinal (GI) tract and central nervous system (CNS). The receptors have a large range of effects in both normal physiology and pathophysiological conditions [5]. GRPRs are normally expressed in nonneuroendocrine tissues of the pancreas, breast, and neuroendocrine cells of the brain, GI tract, lung, and prostate, but are not normally expressed by epithelial cells in the colon, lung, or prostate [6, 7].

Molecular imaging enables the visualization of the cellular function and the followup of the molecular process in living organisms without perturbing them [8]. The radionuclide molecular imaging technique is the most sensitive and can provide target-specific information. The radiotracer could also be used for radionuclide therapy. Thus, the development of a personalized theranostic (image and treat) agent would allow greater accuracy in selection of patients who may respond to treatment, and assessing the outcome of therapeutic response [9]. Gastrin-releasing peptide receptors (GRPRs) are overexpressed in several primary human tumors and metastases [5]. Markwalder and Reubi reported that GRPRs are expressed in invasive prostate carcinomas and in prostatic intraepithelial neoplasms at high

density, whereas normal prostate tissue and hyperplastic prostate tissue were predominantly GRPR negative [10]. These findings suggest that GRPR may be used as a molecular basis for diagnosing and staging prostate cancer, further for imaging-guided personalized medicine using radiolabeled bombesin analogues.

Previous studies have evaluated the ^{111}In-radiolabeled BN analogues which bind rapidly into GRP receptor-positive tumor cells, including PC-3, CA20948, and AR42J using gamma camera imaging after administration [11–14]. AMBA (DO3A-CH$_2$CO-G-(4-aminobenzoyl)-QWAVGHLM-NH$_2$) (Figure 1), a BBN-related peptide agonist, has a DO3A structure that can chelate tripositive lanthanide isotopes, such as ^{68}Ga, ^{90}Y, ^{111}In, and [177]Lu. Thus, it can formulate many kinds of radiolabelled probes for various purposes [15]. Indium 111 emits γ-photons of two energies (172 and 245 keV) as well as Auger and internal conversion electrons. ^{111}In-AMBA was initially used for diagnostic purposes but remains the potential for radiotherapy. Auger electron, with a maximum energy of <30 keV, is a high linear energy transfer (LET) radiation with subcellular pathlength (2–500 nm) in tissues [16]. For imaging the presence or absence of GRPR, the ^{111}In-AMBA could be used for patient selection for further radiotherapy (^{177}Lu-AMBA), chemotherapy (BLP antagonists), or therapeutic response monitoring as imaging-guided personalized medicine. Although ^{111}In-AMBA has been evaluated as an imaging agent [17–20], the pharmacokinetics and dosimetry of the agent have not been reported yet. In this study, ^{111}In-AMBA was designed as an image-guided diagnostic agent for human GRPR-positive tumors, which only retain the last eight amino acids (Q-W-A-V-G-H-L-M-NH$_2$) from native BN. The pharmacokinetics, biodistribution, dosimetry, and micro-SPECT/CT imaging of ^{111}In-AMBA were evaluated in human androgen-independent PC-3 prostate tumor-bearing SCID mice.

2. Materials and Methods

2.1. Chemicals. Protected N$^{\alpha}$-Fmoc-amino acid derivatives were purchased from Calbiochem-Novabiochem (Laufelfingen, Switzerland), Fmoc-amide resin and coupling reagent were purchased from Applied Biosystems Inc. (Foster City, CA, USA), and DOTA-tetra (tBu) ester was purchased from Macrocyclics (Dallas, TX, USA). Fmoc-4-abz-OH was obtained from Bachem (Chauptstrasse, Switzerland). Bombesin was purchased from Fluka (Buchs, Switzerland).

2.2. Synthesis of AMBA. AMBA was synthesized by solid phase peptide synthesis (SPPS) using an Applied Biosystems Model 433A full automated peptide synthesizer (Applied Biosystems, Foster City, CA, USA) employing the Fmoc (9-fluorenylmethoxy-carbonyl) strategy. Carboxyl groups on Fmoc-protected amino acids were activated by (2-(1H-benzotriazol-1-yl)-1,1,3,3-tetramethyluronium hexafluorophosphate (HBTU), forming a peptide bond with the N-terminal amino group on the growing peptide, anchored *via* the C-terminus to the resin, provided for stepwise amino acid addition. Rink Amide resin (0.25 mmole) and Fmoc-protected amino acids (1.0 mmoL), with appropriate side-chain protections, and DOTA-tetra (tBu ester) were used for SPPS of the BBN conjugates. Side chain protecting groups in the synthesis were Trt for Gln and His, and Boc for Trp.

The protected peptide-resin was cleaved and deprotected with mixture of 50% trifluoroacetic acid (TFA): 45% chloroform, 3.75% anisole, and 1.25% 1, 2-ethanedithiol (EDT) for 4 h at room temperature (RT). The crude peptide was isolated by precipitating with cool diethyl ether. After centrifugation, the collected precipitate was dried under vacuum. The crude peptide sample was purified by reverse phase high-performance liquid chromatography (HPLC) using a column of XTerra prep, MSC18, 5 μm, 18 × 50 mm (Waters Corp., MA, USA) with an acetonitrile/water gradient consisting of solvent A (0.1% TFA in H$_2$O) and solvent B (0.1% TFA in acetonitrile), with a 14.8% yield; flow: 6 mL/min; gradient: 20%–40% B for 20 min. The molecular weight was determined with a MALDI-TOF Mass Spectrometer (Bruker Daltonics Inc, Germany). M/z determined for the peptide was AMBA, 1,502.6 [M+H].

2.3. Radiolabeling of ^{111}In-AMBA. AMBA was radiolabeled with ^{111}In as previously described by Zhang et al. [21]. Briefly, AMBA was labeled with [111]In ([111]InCl$_3$, Institute of Nuclear Energy Research (INER), Taoyuan (Taiwan), 16430 MBq/mL in 0.05 N HCl, pH 1.5–1.9) by reaction of 6.66×10^{-4} μmole (1 μg) peptide in 95 μL 0.1 M NH$_4$OAc (pH 5.5) with 64.75 MBq [111]InCl$_3$ in 5 μL 0.04 N HCl for 10 min at 95°C. The specific activity of ^{111}In-AMBA was 9.72×10^4 MBq/μmole. The radiolabeling efficiency was analyzed using instant thin-layer chromatography (ITLC SG, Pall Corporation, New York. USA) with 0.1 M Na-citrate (pH 5.0) as solvent (indium citrate and [111]InCl$_3$: Rf = 0.9~1.0, peptide-bound [111]In: Rf = 0~0.1) [22]. Radio high-performance liquid chromatography (Radio-HPLC) analysis was performed using a Waters 2690 chromatography system with a 2996 photodiode array detector (PDA), a Bioscan radiodetector (Washington, DC, USA), and an FC 203B fraction collector by Gilson (Middleton, WI, USA). ^{111}In-AMBA was purified by an Agilent (Santa Clara, CA, USA) Zorbax bonus-RP HPLC column (4.6 × 250 mm, 5 μm) eluted with a gradient mixture from 10% B to 40% B in 40 min. Flow rate was 1 mL/min at RT, and the retention time for ^{111}In-AMBA was 22.5 min. After purification by HPLC, 100% ethanol was used instead of acetonitrile by solvent exchange with Waters Sep-Pak Light C18 cartridge (Milford, MA, USA). Normal saline was added after evaporation, and pH value was at the range 7~7.5.

2.4. Receptor Cold Competition Assay. Cold competition binding assay was studied using human bombesin 2 receptor expressed in HEK-293 cells as the source of GRP receptors (PerkinElmer, Boston, MA, USA). Assays were performed using FC96 plates and the Multiscreen system (Millipore, Bedford, MA). Binding of ^{125}I-Tyr^4-Bombesin (PerkinElmer,

FIGURE 1: Representative structure of AMBA.

Boston, MA, USA) to human bombesin 2 receptor (0.16 μg per well) was determined in the presence of increasing concentrations (0.001 nmole/L to 1000 nmole/L) of unlabeled AMBA in a buffer solution (20 mmol/L HEPES, pH 7.4, 3 mmol/L $MgCl_2$, 1 mmol/L EDTA, and 0.3% BSA) with a total volume of 250 μL per well. After incubation for 60 min at RT, membranes were filtered and washed with ice-cold Tris-HCl buffer (50 mmol/L). The filters containing membrane-bound radioactivity were counted using a Cobra II gamma-counter (Packard, Meriden, CT). The inhibitory concentration of 50% (IC_{50}) was calculated using a four-parameter curve-fitting routine using the KELL software for Windows version 6 (Biosoft, Ferguson, MO, USA) [13].

2.5. Cell Culture and Animal Model. Human androgen-independent prostate cancer PC-3 cells (Bioresource Collection and Research Center, Taiwan) were cultured in Ham's F-12K medium supplemented with 10% heat-inactivated fetal bovine serum (all from GIBCO, Grand Island, NY, USA) containing 5% CO2 at 37°C. For animal inoculation, an aliquot was thawed, grown and used within 10 passages. Five-week-old male ICR SCID (severely compromised immunodeficient) outbred mice were obtained from the National Animal Center of Taiwan (Taipei, Taiwan, ROC) and maintained on a standard diet (Lab diet; PMI Feeds, St. Louis, MO, USA) at RT, with free access to tap water in the animal house of INER). Thirty-three SCID mice were subcutaneously injected with 2×10^6 PC-3 cells in the right hind flank. The animal experiments were approved by the Institutional Animal Care and Use Committee (IACUC) of the INER.

2.6. Biodistribution Studies. At 4 weeks after PC-3 cell inoculation, the weight of the developed tumors ranged from 0.05 to 0.2 g. Twenty-five PC-3 xenograft SCID mice ($n = 5$ for each group) were injected with 0.37 MBq (0.1 μg) of the ^{111}In-AMBA in 100-μL normal saline via the tail vein. The mice were sacrificed by CO_2 asphyxiation with tissues and organs excised at 1, 4, 8, 24, and 48 h postinjection (p.i.). Subsequently, the tissues and organs were weighed, radioactivity was counted in a Packard Cobra II gamma-counter by Perkin-Elmer (Waltham, MA, USA), and the percentage of injected dose per gram (% ID/g) for each organ or tissue was calculated [23].

2.7. Pharmacokinetic Studies. Six PC-3 xenograft SCID mice were injected with 0.37 MBq (0.1 μg) of the ^{111}In-AMBA in 100-μL normal saline via the tail vein. At 0.25, 1, 4, 16, 24, 48, 72, 96, and 168 h p.i., 20 μL of blood was collected from the heart puncture, then the blood was weighed, radioactivity was counted in the Cobra II gamma-counter, and the percentage of injected dose per gram (% ID/g) was calculated. The data were fitted to a two-compartment model and the pharmacokinetic parameters were derived by the WinNonlin 5.0 software (Pharsight Corporation, Mountain View, CA, USA).

2.8. Micro-SPECT/CT Imaging. Two male SCID mice bearing human PC-3 tumors of approximately 0.1 g were i.v. injected with 12.2 MBq/4 μg ^{111}In-AMBA after purification by radio-HPLC. The SPECT and CT images were acquired by a micro-SPECT/CT scanner system (XSPECT; Gamma Medica-ideas Inc., Northridge, CA, USA). SPECT imaging was performed using medium-energy, parallel-hole collimators at 1, 4, 8, 24, and 48 h. The source and detector were mounted on a circular gantry allowing them to rotate 360 degrees around the subject (mouse) positioned on a stationary bed. The field of view (FOV) was 12.5 cm. The imaging acquisition was accomplished using 64 projections at 90 seconds per projection. The energy windows were set at 173 keV $\pm$ 10% and 247 keV $\pm$ 10%. SPECT imaging was followed by CT imaging (X-ray source: 50 kV, 0.4 mA; 256 projections) with the animal in exactly the same position. A three-dimensional (3D) Feldkamp cone beam algorithm was used for CT image reconstruction, and a two-dimensional (2D) filtered back projection algorithm was used for SPECT image reconstruction. All image processing softwares, including SPECT/CT coregistration, were provided by Gamma Medica-Ideas Inc (Northridge, CA, USA). After coregistration, both the fused SPECT and CT images had 256 $\times$ 256 $\times$ 256 voxels with an isotropic 0.3-mm voxel size.

2.9. Absorbed Radiation Dose Calculations. The relative organ mass scaling method was employed to extrapolate the animal data to humans [24, 25]. The mean absorbed dose in various tissues was calculated from the radionuclide concentration in tissues/organs of interest, assuming a homogeneous distribution of the radionuclide within any source region [26]. The calculated mean value of percentage
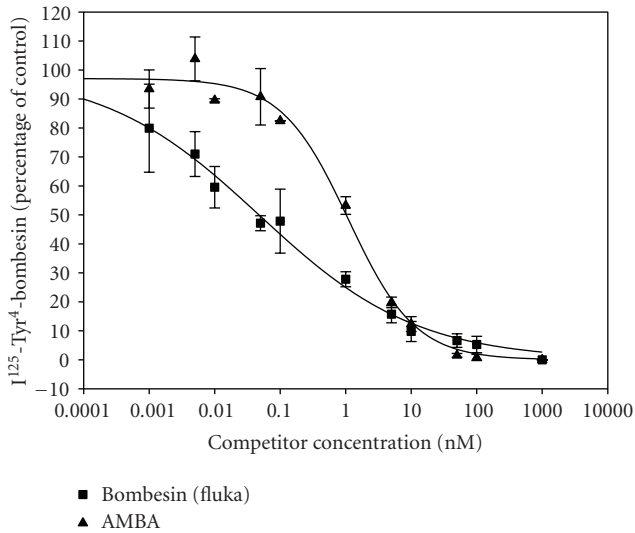
FIGURE 2: Competitive binding assay of AMBA versus ^{125}I-Tyr^4-Bombesin with human bombesin 2 receptors.

of injected activity per g (% IA/g) for the organs in mice was extrapolated to uptake in organs of a 70-kg adult using the following formula [24]:

$$\left[\left(\frac{\%\text{IA}}{g_{\text{organ}}} \right)_{\text{animal}} \times \left(\text{Kg}_{\text{TB weight}} \right)_{\text{animal}} \right] \times \left(\frac{g_{\text{organ}}}{\text{Kg}_{\text{TB weight}}} \right)_{\text{human}}$$
$$= \left(\frac{\%\text{IA}}{\text{organ}} \right)_{\text{human}}. \tag{1}$$

The extrapolated values (% IA) in the human organs at 1, 4, 8, 24, and 48 h were fitted with exponential biokinetic models and integrated to obtain the number of disintegrations in the source organs. This information was entered into the OLINDA/EXM computer program. The integrals (MBq-s) for 15 organs, including heart contents (blood), brain, muscle, bone, heart, lung, spleen, pancreas, kidneys, liver, and remainder of body were evaluated and used for dosimetry evaluation. The code also displays contributions of different source organs to the total dose of target organs. For the estimation of the tumor absorbed dose, it was assumed that once the radiopharmaceutical is inside the tumor, there is no biological elimination.

3. Results

3.1. Radiolabeling and In Vitro Receptor Binding Assay. The radiolabeling efficiency of ^{111}In-AMBA was 95.43 $\pm$ 1.37% ($n = 11$). The *in vitro* competitive binding assays were determined in the human bombesin 2 receptor using ^{125}I-Tyr^4-Bombesin as the GRP-R specific radiotracer, and unlabeled AMBA and native BN as competitors. The IC$_{50}$ of the AMBA and native BN in human bombesin 2 receptor (Figure 2) is 0.82 $\pm$ 0.41 nmol/L and 0.13 $\pm$ 0.10 nmol/L, respectively, in a single, direct, nanomolar range, demonstrating high specificity and affinity for the GRP receptor.

The Ki of AMBA and native BBN were 0.65 $\pm$ 0.32 nmol/L and 0.10 $\pm$ 0.08 nmol/L, respectively.

3.2. Biodistribution. ^{111}In-AMBA accumulated significantly in tumor, adrenal, pancreas, small intestine, and large intestine (Table 1). Fast blood clearance and fast excretion from the kidneys were observed. High levels of radioactivity were found in the kidneys before 24 h, indicating that the radioactivity was excreted rapidly in the urine within 24 h. The levels of radioactivity reached the highest with 3.87 $\pm$ 0.65 % ID/g at 8 h and then declined rapidly. The highest tumor/muscle ratio (Tu/Mu) of ^{111}In-AMBA was 11.79 at 8 h after injection and decreased progressively to 4.82 and 5.16 at 24 and 48 h after administration, respectively. Other GRPR-positive organs (small intestine and large intestine) also showed the specific binding of ^{111}In-AMBA (Table 1). The tumor/muscle ratios were decreased conspicuously at 4 and 24 h postadministration.

3.3. Pharmacokinetic Studies. The radioactivity declined to under detection limit after 24 h. The pharmacokinetic parameters derived by a two-compartment model [27] indicated that the distribution half-life ($t_{1/2\alpha}$) and distribution half-life ($t_{1/2\beta}$) of ^{111}In-AMBA were 1.53 $\pm$ 0.69 h and 30.73 $\pm$ 8.56 h, respectively (Table 2).

3.4. Micro-SPECT/CT Imaging. Micro-SPECT/CT imaging of ^{111}In-AMBA indicated significant uptake in the tumors at 8 and 24 h after intravenous injection (Figure 3). The longitudinal micro-SPECT/CT imaging showed high accumulation of ^{111}In-AMBA in pancreas and gastrointestinal tract at 4, 8, 24, and 48 h after intravenous injection.

3.5. Radiation Absorbed Dose Calculation. The radiation-absorbed dose projections for the administration of ^{111}In-AMBA to humans, determined from the residence times in mice, are shown in Table 3. The highest absorbed doses appear in the lower large intestine (0.12 mSv/MBq^{-1}), upper large intestine (0.13 mSv/MBq^{-1}), kidneys (0.12 mSv/MBq^{-1}), osteogenic cells (0.22 mSv/MBq^{-1}), and pancreas (0.25 mSv/MBq^{-1}). The effective dose appears to be approximately m0.11 mSv/MBq^{-1}. The red marrow absorbed dose is estimated to be 0.09 mSv/MBq^{-1}. For a 2-g tumor, the unit density sphere model was used and the estimated absorbed dose was 8.09 mGy·MBq^{-1}.

4. Discussion

Growth factor receptors are involved in all steps of tumor progression, enhancing angiogenesis, local invasion, and distant metastases. The overexpression of growth factor receptors on the cell surface of malignant cells might be associated with a more aggressive behavior and a poor prognosis. For these reasons, tumor-related growth factor receptors can be taken as potential targets for therapeutic intervention. Over the last two decades, GRP and other BLPs may act as a growth factor in many types of cancer. GRPR antagonists have been developed as anticancer candidate
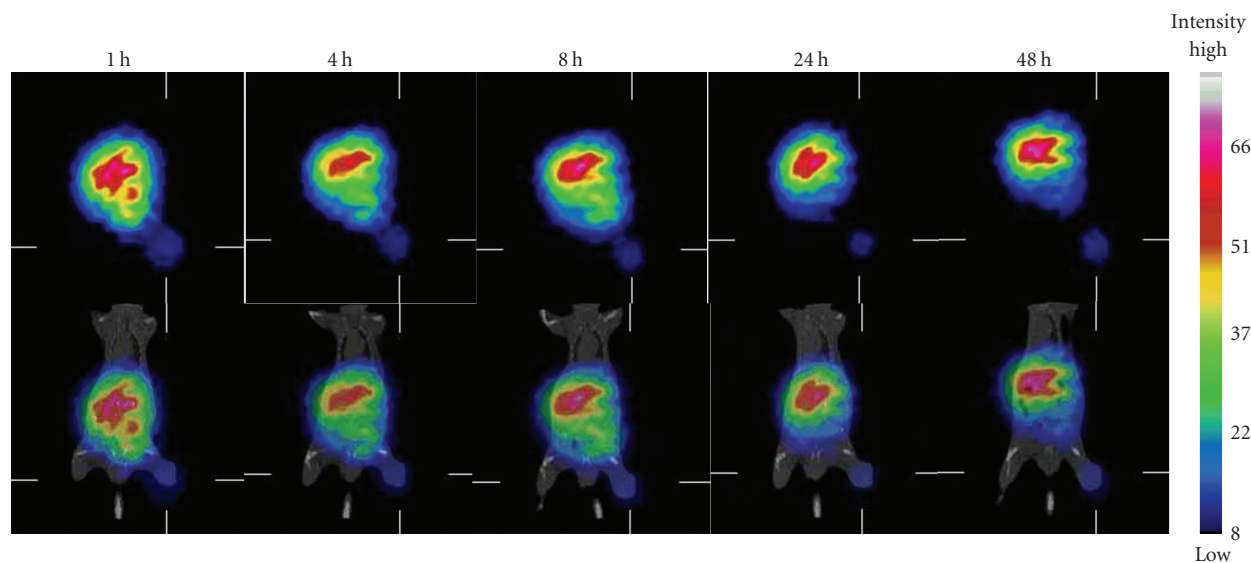
FIGURE 3: MicroSPECT/CT images of ^{111}In-AMBA targeting PC-3 tumors xenograft SCID mice. 12.2 MBq/4 μg ^{111}In-AMBA was administered to each mouse by intravenous injection. The images were acquired at 1, 4, 8, 24, and 48 h after injection. The energy window was set at 173 keV ± 10% and 247 keV ± 10%; the image size was set at 80 × 80 pixels. The color map shows the SPECT pixel values from 0 to the maximum expressed with an arbitrary value of 100.

TABLE 1: Biodistribution of ^{111}In-AMBA after intravenous injection in PC-3 prostate tumor-bearing SCID mice.

Organ	1 h	4 h	8 h	24 h	48 h
Blood	0.95 ± 0.09	0.50 ± 0.06	0.42 ± 0.02	0.19 ± 0.03	0.09 ± 0.02
Brain	0.06 ± 0.01	0.05 ± 0.01	0.05 ± 0.00	0.02 ± 0.00	0.03 ± 0.00
Skin	0.99 ± 0.22	0.60 ± 0.16	0.55 ± 0.02	0.36 ± 0.02	0.28 ± 0.02
Muscle	0.57 ± 0.19	0.33 ± 0.14	0.33 ± 0.02	0.21 ± 0.04	0.14 ± 0.02
Bone	1.02 ± 0.18	0.92 ± 0.21	1.57 ± 0.18	0.90 ± 0.13	0.60 ± 0.07
Heart	0.62 ± 0.09	0.48 ± 0.04	0.56 ± 0.08	0.41 ± 0.05	0.32 ± 0.04
Lung	1.78 ± 0.23	1.88 ± 0.46	1.70 ± 0.65	0.60 ± 0.17	0.26 ± 0.03
Adrenals	5.79 ± 1.21	7.08 ± 1.22	17.8 ± 4.65	7.41 ± 1.99	5.20 ± 1.11
Spleen	2.80 ± 1.49	6.90 ± 1.87	8.90 ± 2.34	4.41 ± 0.58	2.19 ± 0.51
Pancreas	6.14 ± 0.99	12.9 ± 2.44	54.9 ± 2.51	15.9 ± 1.94	9.80 ± 2.21
Kidney	3.56 ± 0.15	4.23 ± 0.28	3.92 ± 0.91	4.10 ± 0.72	2.74 ± 0.30
Liver	7.26 ± 0.53	8.22 ± 1.05	7.04 ± 0.24	8.64 ± 1.31	6.59 ± 1.83
Bladder	7.63 ± 2.94	1.75 ± 0.75	1.07 ± 0.12	0.64 ± 0.06	0.46 ± 0.10
Stomach	0.81 ± 0.09	0.80 ± 0.07	3.97 ± 1.15	0.97 ± 0.29	0.47 ± 0.05
SI	1.67 ± 0.22	1.56 ± 0.17	4.42 ± 0.61	1.48 ± 0.27	0.74 ± 0.10
LI	1.77 ± 0.25	3.42 ± 1.10	7.04 ± 1.48	2.39 ± 0.38	0.99 ± 0.16
Tumor (PC-3)	2.24 ± 0.66	1.86 ± 0.71	3.87 ± 0.65	1.02 ± 0.09	0.75 ± 0.08
Tumor/muscle	3.89	5.69	11.79	4.82	5.16

Values are expressed as % ID/g, mean ± SEM (n = 4-5 at each time point). SI: small intestine; LI: large intestine.

compounds, exhibiting impressive antitumoral activity both *in vitro* and *in vivo* in various murine and human tumors [28, 29]. Clinical trials with GRPR antagonists in cancer patients are in its initial phase as anticipated by animal toxicology studies and preliminary evaluation in humans [29]. Presently, efforts at the identification of the most suitable candidates for clinical trials and at improving drug formulation for human use are considered priorities. It may also be anticipated that GRPRs may be exploited as

potential carriers for cytotoxins, immunotoxins, or radioactive compounds. Thus, the visualization of these receptors through molecular image-guided diagnostic agents may become an interesting tool for tumor detection and staging in personalized medicine.

The present study showed the highest accumulation of ^{111}In-AMBA in pancreas in mice (Table 1). However, interspecies differences in structure and pharmacology of human and animal GRP receptors have been reported [30].

Table 2: Pharmacokinetic parameters of plasma in PC-3 tumor-bearing mice after intravenous injection of $10\,\mu\text{Ci/mouse}$ ^{111}In-AMBA (mean $\pm$ SEM, $n = 5$).

Parameter	Unit	Value
A	% ID/g	6.15 ± 0.69
B	% ID/g	1.43 ± 0.61
α	1/h	1.19 ± 0.85
β	1/h	0.03 ± 0.01
$\text{AUC}_{0-168\text{h}}$	$\text{h} \times (\% \text{ID/g})$	66.4 ± 17.3
$t_{1/2\alpha}$	h	1.53 ± 0.69
$t_{1/2\beta}$	h	30.7 ± 8.56
$C_{\max}$	% ID/g	7.37 ± 0.64

A, B, α, β: macro rate constants; $t_{1/2\alpha}$, $t_{1/2\beta}$: distribution and elimination half-lives; $\text{AUC}_{0-168\text{h}}$: area under concentration of ^{111}In-AMBA versus time curve; $C_{\max}$: maximum concentration in plasma.

Table 3: Radiation dose estimates for ^{111}In-AMBA in humans.

Organ	Estimated dose (mSv/MBq^{-1})*
Adrenals	$1.5E-01$
Brain	$3.1E-02$
Breasts	$7.7E-02$
Gallbladder Wall	$1.5E-01$
LLI Wall	$1.2E-01$
Small Intestine	$1.3E-01$
Stomach Wall	$1.1E-01$
ULI Wall	$1.3E-01$
Heart Wall	$7.2E-02$
Kidneys	$1.2E-01$
Liver	$2.0E-01$
Lungs	$7.4E-02$
Muscle	$7.0E-02$
Ovaries	$1.2E-01$
Pancreas	$2.5E-01$
Red Marrow	$8.8E-02$
Osteogenic Cells	$2.2E-01$
Skin	$5.8E-02$
Spleen	$1.2E-01$
Testes	$5.9E-02$
Thymus	$9.0E-02$
Thyroid	$9.2E-02$
Urinary Bladder Wall	$1.1E-01$
Uterus	$1.3E-01$
Total Body	$9.2E-02$
Effective Dose	$1.1E-01$

*Radiation-absorbed dose projections in humans were determined from residence times for ^{111}In-AMBA in SCID mice and were calculated by use of OLINDA/EXM version 1.0 computer program.

Because the pancreas is the primary normal tissue in these animals that expresses a high density of bloodstream-accessible GRPRs, the accumulation of ^{111}In in the pancreas is a direct reflection of the efficacy of radiolabeled BN analogs for *in vivo* targeting of cell-surface-expressed GRPRs [31]. Retention of ^{111}In-AMBA in the pancreas may be due to the

characteristic of a radioagonist with effective internalization and cell retention. Waser et al. reported that in contrast to the strongly labeled GRPR-positive mouse pancreas with ^{177}Lu-AMBA, the human pancreas did not bind ^{177}Lu-AMBA unless chronic pancreatitis was diagnosed [32].

The majority of research efforts into the design of bombesin-based radiopharmaceuticals have been carried out using GRPR agonists. The main reason for using agonists is that they undergo receptor-mediated endocytosis enabling residualization of the attached radiometal within the targeted cell [33]. Micro-SPECT/CT imaging is a noninvasive imaging modality that can longitudinally monitor the behavior of GRPR expression in the same animal across different time-points before and during therapy. In the present study, tumor targeting and localization of ^{111}In-AMBA was clearly imaged with micro-SPECT/CT after 1 to 48 h of administration, suggesting that micro-SPECT/CT imaging with ^{111}In-AMBA is a good tool for studying the tumor targeting, distribution, and real-time therapeutic response *in vivo*.

The effective dose projected for the administration of ^{111}In-AMBA to humans (0.11 mSv/MBq^{-1}) (Table 3) is comparable to that for ^{111}In-pentetreotide (0.12 mSv/MBq^{-1}) [34], the only ^{111}In-labeled peptide receptor-targeted radio-therapeutic agent to be used clinically [35, 36]. The intestines, osteogenic cells, kidneys, and pancreas appear to receive absorbed doses around 0.2 mSv/MBq^{-1} of ^{111}In-AMBA. At a maximum planned administration of 111 MBq for diagnostic imaging, the total radiation-absorbed dose to these organs kidneys would be about 12 mSv. The use of animal data to estimate human doses is a necessary first step, but such studies give only an estimate of radiation doses to be expected in human subjects. More accurate human dosimetry must be established with imaging studies involving human volunteers or patients. The dosimetry data presented here will be valuable in the dose planning of these studies, and for application of ^{111}In-AMBA to Investigational New Drug (IND) research.

Clinically, primary prostate cancer and the metastases may be heterogeneous, demonstrating a spectrum of phenotypes from androgen-sensitive to androgen-insensitive. ^{177}Lu-AMBA, a conjugated bombesin compound for imaging and systemic radiotherapy, is now in phase I clinical trials [15]. ^{177}Lu-AMBA has been evaluated in early stages of prostate cancer represented by the androgen-dependent, prostate-specific antigen-secreting hormone-sensitive prostate cancer cell line LNCaP [6], derived from a lymph node metastasis, and also in PC-3 cell line, derived from bone metastasis, is androgen-independent and is thought to represent late-stage hormone-refractory prostate cancer (HRPC) [37]. ^{177}Lu-AMBA will be clinically efficacious as a single-agent radiotherapeutic for heterogeneous metastatic prostate cancer and be a valuable adjunct to traditional chemotherapy. Thus, the visualization of GRPR receptors through ^{111}In-AMBA as an image-guided agent may contribute to the use of radiotherapeutic, ^{177}Lu-AMBA, and other traditional chemotherapy in personalized medicine.

Targeted therapeutic and imaging agents are becoming more prevalent and are used to treat increasingly smaller

population of patients. This has led to dramatic increases in the costs for clinical trials. Biomarkers have great potential to reduce the numbers of patients needed to test novel targeted agents by predicting or identifying nonresponse early on and thus enriching the clinical trial population with patients more likely to respond. GRPRs are expressed on prostate tumor cells, making it a potential biomarker for cancer. The imaging of ^{111}In-AMBA indicated the stage of prostate cancer for determining the therapeutic approach to prostate cancer and for monitoring the therapeutic efficacy. The expression of GRPR will vary from patient to patient due to the stages and individual difference. If such patients could be prescreened with ^{111}In-AMBA to identify those with higher tumor expression of GRPR, then it would be possible to select cases for receiving BLPs-specific treatment, while cases with low tumor expression of GRPR can consider other treatment options. Consequently, the proposed approaches enable optimized and individualized treatment protocols and can enhance the development of image-guide personalized medicine.

By visualizing how well drug targeting systems deliver pharmacologically active agents to the pathological site, ^{111}In-AMBA furthermore facilitates "personalized medicine" and patient individualization, as well as the efficacy of combination regimens. Regarding personalized medicine, it can be reasoned that only in patients showing high levels of target site uptake with high expression of GRPR should treatment be continued; otherwise, alternative therapeutic approaches should be considered.

5. Conclusion

^{111}In-AMBA showed a characteristic of agonist, a good bioactivity *in vitro* and uptake in human GRPR-expressing tumors *in vivo*. The molecular image-guided diagnostic agent can be used for various different purposes, ranging from simple and straightforward biodistribution studies to extensive and elaborate experimental setups aiming to enable "personalized medicine" and to improve the efficacy of combined modality anticancer therapy.

Acknowledgments

References

[1] A. Jemal, R. Siegel, E. Ward, Y. Hao, J. Xu, and M. J. Thun, "Cancer statistics, 2009," *CA Cancer Journal for Clinicians*, vol. 59, no. 4, pp. 225–249, 2009.

[2] V. Erspamer, G. F. Erpamer, and M. Inselvini, "Some pharmacological actions of alytesin and bombesin," *Journal of Pharmacy and Pharmacology*, vol. 22, no. 11, pp. 875–876, 1970.

[3] G. S. Kroog, R. T. Jensen, and J. F. Battey, "Mammalian bombesin receptors," *Medicinal Research Reviews*, vol. 15, no. 5, pp. 389–417, 1995.

[4] H. Ohki-Hamazaki, M. Iwabuchi, and F. Maekawa, "Development and function of bombesin-like peptides and their receptors," *International Journal of Developmental Biology*, vol. 49, no. 2-3, pp. 293–300, 2005.

[5] R. T. Jensen, J. F. Battey, E. R. Spindel, and R. V. Benya, "International union of pharmacology. LXVIII. Mammalian bombesin receptors: nomenclature, distribution, pharmacology, signaling, and functions in normal and disease states," *Pharmacological Reviews*, vol. 60, no. 1, pp. 1–42, 2008.

[6] M. E. Maddalena, J. Fox, J. Chen et al., "Lu-AMBA biodistribution, radiotherapeutic efficacy, imaging, and autoradiography in prostate cancer models with low GRP-R expression," *Journal of Nuclear Medicine*, vol. 50, no. 12, pp. 2017–2024, 2009.

[7] A. Nagy and A. V. Schally, "Targeting cytotoxic conjugates of somatostatin, luteinizing hormone-releasing hormone and bombesin to cancers expressing their receptors: a "smarter" chemotherapy," *Current Pharmaceutical Design*, vol. 11, no. 9, pp. 1167–1180, 2005.

[8] J. K. Willmann, N. van Bruggen, L. M. Dinkelborg, and S. S. Gambhir, "Molecular imaging in drug development," *Nature Reviews Drug Discovery*, vol. 7, no. 7, pp. 591–607, 2008.

[9] T. Lammers, F. Kiessling, W. E. Hennink, and G. Storm, "Nanotheranostics and image-guided drug delivery: current concepts and future directions," *Molecular Pharmaceutics*, vol. 7, no. 6, pp. 1899–1912, 2010.

[10] R. Markwalder and J. C. Reubi, "Gastrin-releasing peptide receptors in the human prostate: relation to neoplastic transformation," *Cancer Research*, vol. 59, no. 5, pp. 1152–1159, 1999.

[11] C.-L. Ho, L.-C. Chen, W.-C. Lee et al., "Receptor-binding, biodistribution, dosimetry, and micro-SPECT/CT imaging of [111]In-[DTPA^1, Lys^3, Tyr^4]-bombesin analog in human prostate tumor-bearing mice," *Cancer Biotherapy and Radiopharmaceuticals*, vol. 24, no. 4, pp. 435–443, 2009.

[12] W. A. P. Breeman, M. De Jong, B. F. Bernard et al., "Preclinical evaluation of [^{111}In-DTPA-Pro^1, Tyr^4]bombesin, a new radioligand for bombesin-receptor scintigraphy," *International Journal of Cancer*, vol. 83, no. 5, pp. 657–663, 1999.

[13] W. A. P. Breeman, M. De Jong, J. L. Erion et al., "Preclinical comparison of In-labeled DTPA- or DOTA-bombesin analogs for receptor-targeted scintigraphy and radionuclide therapy," *Journal of Nuclear Medicine*, vol. 43, no. 12, pp. 1650–1656, 2002.

[14] M. De Visser, H. F. Bernard, J. L. Erion et al., "Novel ^{111}In-labelled bombesin analogues for molecular imaging of prostate tumours," *European Journal of Nuclear Medicine and Molecular Imaging*, vol. 34, no. 8, pp. 1228–1238, 2007.

[15] M. F. Tweedle, "Peptide-targeted diagnostics and radiotherapeutics," *Accounts of Chemical Research*, vol. 42, no. 7, pp. 958–968, 2009.

[16] J. G. Kereiakes and D. V. Rao, "Auger electron dosimetry: report of AAPM Nuclear Medicine Committee Task Group No. 6," *Medical Physics*, vol. 19, no. 6, pp. 1359–1360, 1992.

[17] I.-H. Liu, C.-H. Chang, C.-L. Ho et al., "Multimodality imaging and preclinical evaluation of ^{177}Lu-AMBA for human prostate tumours in a murine model," *Anticancer Research*, vol. 30, no. 10, pp. 4039–4048, 2010.

[18] J. C. Garrison, T. L. Rold, G. L. Sieckman et al., "Evaluation of the pharmacokinetic effects of various linking group using the ^{111}In-DOTA-X-BBN(7-14)NH structural paradigm in a prostate cancer model," *Bioconjugate Chemistry*, vol. 19, no. 9, pp. 1803–1812, 2008.

[19] R. P. J. Schroeder, C. Müller, S. Reneman et al., "A standardised study to compare prostate cancer targeting efficacy of five radiolabelled bombesin analogues," *European Journal of Nuclear Medicine and Molecular Imaging*, vol. 37, no. 7, pp. 1386–1396, 2010.

[20] R. Mansi, X. Wang, F. Forrer et al., "Evaluation of a 1,4,7,10-tetraazacyclododecane-1,4,7,10-tetraacetic acid-conjugated bombesin-based radioantagonist for the labeling with single-photon emission computed tomography, positron emission tomography, and therapeutic radionuclides," *Clinical Cancer Research*, vol. 15, no. 16, pp. 5240–5249, 2009.

[21] H. Zhang, J. Chen, C. Waldherr et al., "Synthesis and evaluation of bombesin derivatives on the basis of pan-bombesin peptides labeled with Indium-111, Lutetium-177, and Yttrium-90 for targeting bombesin receptor-expressing tumors," *Cancer Research*, vol. 64, no. 18, pp. 6707–6715, 2004.

[22] W. H. Bakker, R. Albert, C. Bruns et al., "[^{111}In-DTPA-D-Phe^1]-octreotide, a potential radiopharmaceutical for imaging of somatostatin receptor-positive tumors: synthesis, radiolabeling and in vitro validation," *Life Sciences*, vol. 49, no. 22, pp. 1583–1591, 1991.

[23] C. J. Smith, H. Gali, G. L. Sieckman et al., "Radiochemical investigations of ^{177}Lu-DOTA-8-Aoc-BBN[7-14]NH: an in vitro/in vivo assessment of the targeting ability of this new radiopharmaceutical for PC-3 human prostate cancer cells," *Nuclear Medicine and Biology*, vol. 30, no. 2, pp. 101–109, 2003.

[24] M. G. Stabin and J. A. Siegel, "Physical models and dose factors for use in internal dose assessment," *Health Physics*, vol. 85, no. 3, pp. 294–310, 2003.

[25] E. M. Molina-Trinidad, C. A. D. Murphy, G. Ferro-Flores, E. Murphy-Stack, and H. Jung-Cook, "Radiopharmacokinetic and dosimetric parameters of ^{188}Re-lanreotide in athymic mice with induced human cancer tumors," *International Journal of Pharmaceutics*, vol. 310, no. 1-2, pp. 125–130, 2006.

[26] International Commission on Radiological Units and Measurements, "Absorbed-Dose Specification in Nuclear Medicine, ICRU Report 67," *Journal of the ICRU*, vol. 2, no. 1, 2002.

[27] C. H. Chang, TA. K. Chou, C. Y. Yang, T. J. Chang, YU. H. Wu, and TE. W. Lee, "Biodistribution and pharmacokinetics of transgenic pig-produced recombinant human factor IX (rhFIX) in rats," *In Vivo*, vol. 22, no. 6, pp. 693–698, 2008.

[28] S. Sotomayor, L. Muñoz-Moreno, M. J. Carmena et al., "Regulation of HER expression and transactivation in human prostate cancer cells by a targeted cytotoxic bombesin analog (AN-215) and a bombesin antagonist (RC-3095)," *International Journal of Cancer*, vol. 127, no. 8, pp. 1813–1822, 2010.

[29] D. B. Cornelio, R. Roesler, and G. Schwartsmann, "Gastrin-releasing peptide receptor as a molecular target in experimental anticancer therapy," *Annals of Oncology*, vol. 18, no. 9, pp. 1457–1466, 2007.

[30] T. Maina, B. A. Nock, H. Zhang et al., "Species differences of bombesin analog interactions with GRP-R define the choice of animal models in the development of GRP-R-targeting drugs," *Journal of Nuclear Medicine*, vol. 46, no. 5, pp. 823–830, 2005.

[31] J. L. Scemama, A. Zahidi, and D. Fourmy, "Interaction of [^{125}I]-Tyr-bombesin with specific receptors on normal human pancreatic membranes," *Regulatory Peptides*, vol. 13, no. 2, pp. 125–132, 1986.

[32] B. Waser, V. Eltschinger, K. Linder, A. Nunn, and J. C. Reubi, "Selective in vitro targeting of GRP and NMB receptors in human tumours with the new bombesin tracer Lu-AMBA," *European Journal of Nuclear Medicine and Molecular Imaging*, vol. 34, no. 1, pp. 95–100, 2007.

[33] C. J. Smith, W. A. Volkert, and T. J. Hoffman, "Radiolabeled peptide conjugates for targeting of the bombesin receptor superfamily subtypes," *Nuclear Medicine and Biology*, vol. 32, no. 7, pp. 733–740, 2005.

[34] S. Louis, "Octreoscan kit for the preparation of indium-111 pentetreotide [product monograph]," 1995.

[35] M. Ferrari, M. Cremonesi, M. Bartolomei et al., "Dosimetric model for locoregional treatments of brain tumors with Y-conjugates: clinical application with Y-DOTATOC," *Journal of Nuclear Medicine*, vol. 47, no. 1, pp. 105–112, 2006.

[36] E. P. Krenning, P. P. M. Koolj, W. H. Bakker et al., "Radiotherapy with a radiolabeled somatostatin analogue, [^{111}In-DTPA-D-Phe^1]-Octreotide. A case history," *Annals of the New York Academy of Sciences*, vol. 733, pp. 496–506, 1994.

[37] L. E. Lantry, E. Cappelletti, M. E. Maddalena et al., "^{177}Lu-AMBA: synthesis and characterization of a selective ^{177}Lu-labeled GRP-R agonist for systemic radiotherapy of prostate cancer," *Journal of Nuclear Medicine*, vol. 47, no. 7, pp. 1144–1152, 2006.